



Title	High Power CO ₂ Laser Cutting and Welding of Ceramics(Physics, Process, Instrument & Measurement)
Author(s)	Tomie, Michio; Abe, Nobuyuki; Noguchi, Shuichi et al.
Citation	Transactions of JWRI. 1989, 18(1), p. 37-41
Version Type	VoR
URL	https://doi.org/10.18910/12638
rights	
Note	

The University of Osaka Institutional Knowledge Archive : OUKA

<https://ir.library.osaka-u.ac.jp/>

The University of Osaka

High Power CO₂ Laser Cutting and Welding of Ceramic†

Michio TOMIE*, Nobuyuki ABE*, Shuichi NOGUCHI**, Tatsuharu ODA*** and Yoshiaki ARATA****

Abstract

A new combination nozzle which allows dross-free laser cutting of ceramics and other materials was developed, enabling fine cutting of up to 6 mm. A new method of plasma control for welding ceramics was also developed, enabling full penetration welds of alumina ceramics up to 10 mm thick in a high temperature furnace.

KEY WORDS: (High Power CO₂ Laser) (Laser Cutting) (Laser Welding) (Alumina Ceramics) (Cutting Nozzle) (Deep Penetration) (Dross)

1. Introduction

Ceramics are superior to other materials in terms of heat resistance, corrosion resistance, and wear resistance. After metals and plastics, ceramics are expected to be the third most important material for supporting future technological innovation. However, since ceramics are hard and brittle, they are difficult to process as compared to metals.

Ceramics generally have high melting points, so they can only be heat-processed by high energy density heat sources such as lasers or electron beams. Past experiments in welding, cutting and drilling of ceramics with lasers and electron beams¹⁻⁵⁾ have all employed powers of less than 1 kW on thin specimens only millimeters thick.

In this report, in order to study the heat processing of thicker ceramics, the welding and cutting characteristics of ceramics having various alumina contents were investigated using a high power CO₂ laser.

2. Experimental Procedures

As the heat source for cutting and welding, a 15 kW CO₂ laser (beam outer diameter 70 mm, module 1.5) and the Arata laser focusing system (A and C types)⁶⁾ were used. The A type, which was used for welding, employs a focusing system of F 10 with a spot diameter of approximately 0.8 mm. The C type, which was used for both cutting and welding, employs a focusing system of F 4.5 with a spot diameter of approximately 0.4 mm. (Spot

diameter: the diameter at 1/e of the highest value of the beam intensity profile)

For cutting, a combination nozzle was used which was made by joining a coaxial gas nozzle with a dross blowout nozzle. The coaxial gas nozzle was designed so as to blow gas onto the specimen from the front and rear in relation to the point of laser irradiation. A diagram and photograph of this combination nozzle is shown in Fig. 1.

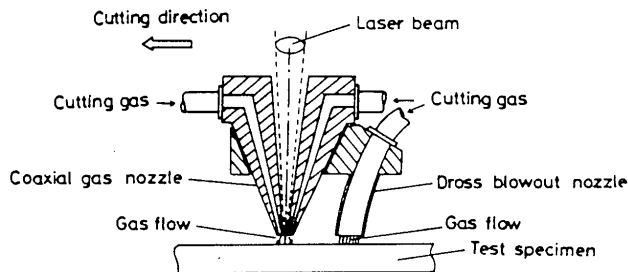
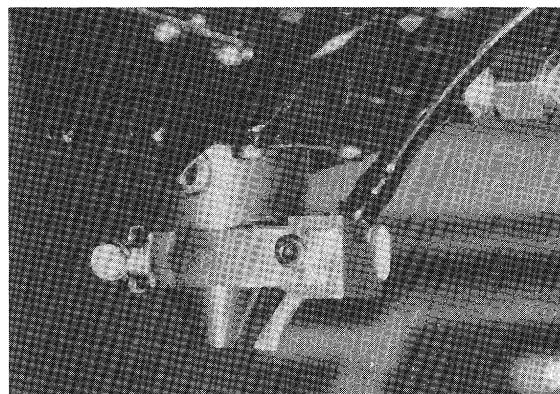


Fig. 1 Schematic diagram of combination nozzle for cutting.

† Received on May 8, 1989

* Associate Professor

** Researcher, Osaka Prefectural Industrial Technology Research Institute

*** Researcher

**** Emeritus Professor, Professor of Kinki University

Because the resistance of ceramics to thermal shock is very small, the specimen was held between firebricks and preheated with a gas burner. The focal position of the laser beam for cutting was set at the surface of the specimen ($a_b = 1.000$).

For welding, a plasma cutting nozzle⁷⁾ was used. A shielding nozzle was used to shield the laser beam from ceramic vapor and gas. A diagram and photograph of this plasma cutting nozzle is shown in Fig. 2. A furnace for welding was made from firebricks, with a gas burner inserted into the side of the furnace. The specimen was

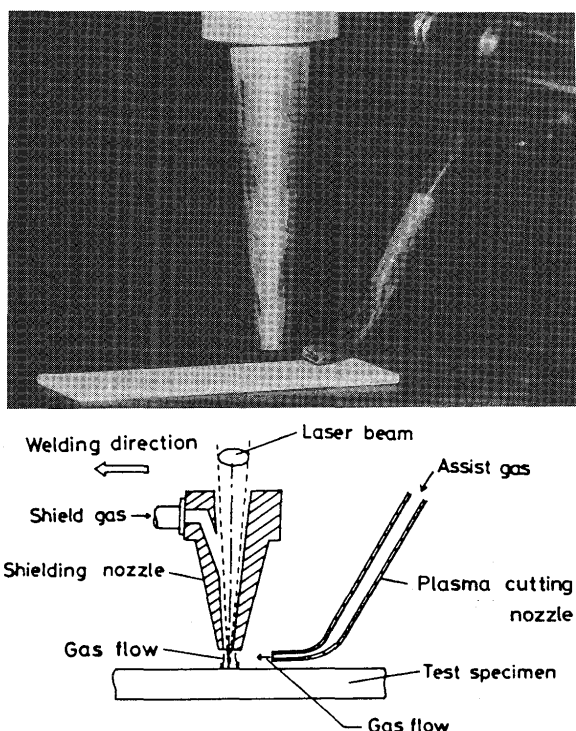


Fig. 2 Schematic diagram of plasma cutting nozzle for welding.

Table 1 Chemical composition and physical constants of Al_2O_3 ceramics used.

			87% Al_2O_3	76% Al_2O_3
Chemical composition	Al_2O_3	%	87	76
	Others		SiO ₂ 10% MgO 2% CaO	SiO ₂ 10% ZrO ₂ 12% CaO, MgO Fe ₂ O ₃ , Na ₂ O
Apparent density		g/cm ³	3.4	3.6
Vickers hardness (500g)		—	1,300	1,000
Bending strength		kg/mm ²	30	.16
Coefficient of thermal expansion (40~800°C)		1/°C ($\times 10^{-6}$)	7.8	7.1
Heat conductivity (20°C)		$\frac{cal \cdot cm}{cm^2 \cdot sec \cdot ^\circ C}$	0.03	0.02
Specific heat		cal/g°C	0.18	0.18

preheated from the back and furnace welding was then conducted. The upper part of the furnace was open, with the furnace designed so as to allow the nozzle to travel inside the furnace. After welding the specimen was cooled in the furnace. The chemical composition and physical constants of the ceramic specimen used in this experiment are shown in Table 1. The alumina content was 87% and 76% (indicated as 87% Al_2O_3 , 76% Al_2O_3). The specimen size was 20 mm wide \times 80 mm long, with a thickness of 2–10 mm.

3. Results and Discussion

3.1 Laser cutting

The high viscosity coefficient of molten ceramic results in poor mobility and in clinging of dross to the back of the specimens, so it is very difficult to achieve fine laser cutting of ceramics. Figure 3 shows the results of ceramic cutting with a conventional coaxial gas nozzle only.

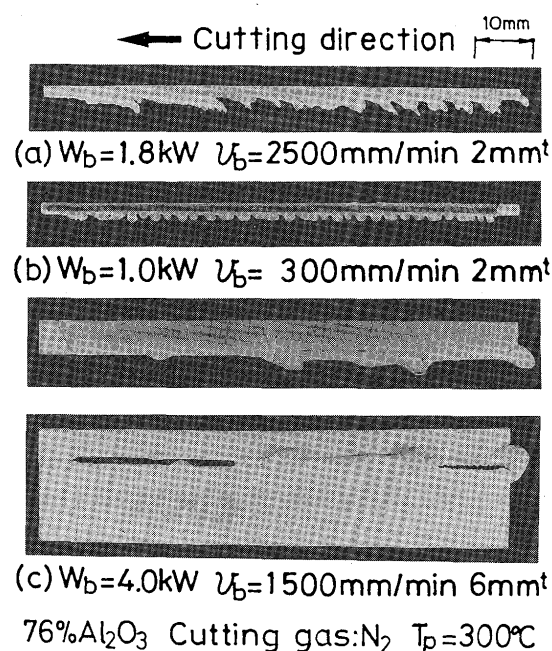


Fig. 3 Cut appearance after conventional cutting.

Although many trials were performed using various combinations of laser power and cutting speed, dross clung under all conditions, making fine cutting impossible.

In order to eliminate dross, a dross blowout nozzle was employed. Fig. 4 shows the laser cutting phenomena of ceramics using a combination nozzle. Figure 4(a) is a photograph taken at the time cutting was begun. Figure 4(b) was taken 0.5 seconds after cutting began and shows the effect of the dross blowout nozzle. Figure 4(c) shows cutting in a steady state. Ceramic melted by the laser beam is blown out of the front bottom of the kerf as

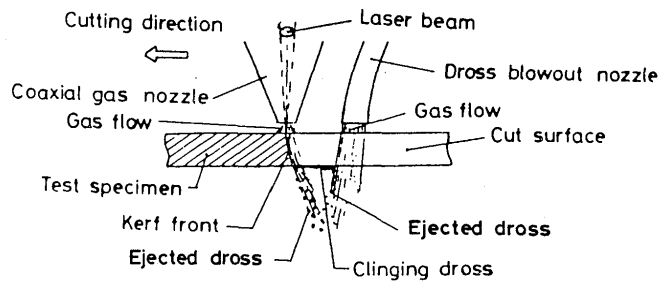
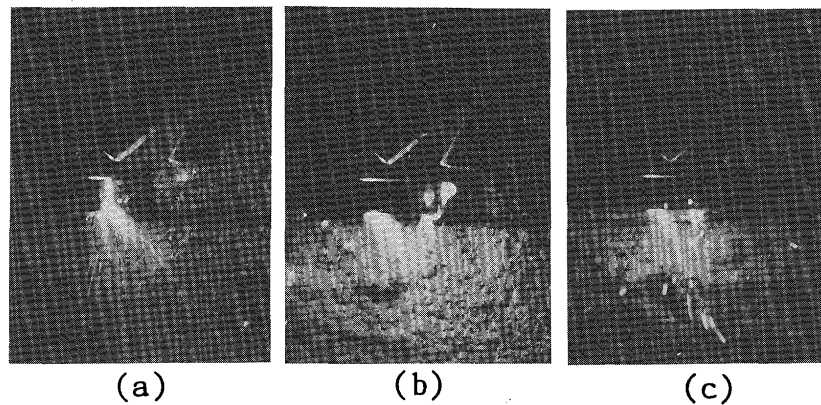


Fig. 4 Appearance of dross ejected by a combination nozzle (a) at the start of cutting, (b) after 0.5 sec, (c) steady state cutting.

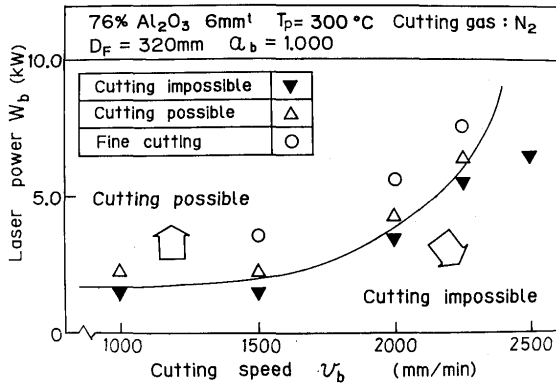


Fig. 5 Relationship between cutting speed and laser power for 6 mm thick 76% Al_2O_3 .

ejected dross. To prevent clinging of the dross which normally flows along the bottom edge of the kerf, it is blown out as ejected dross by injection gas from the dross blowout nozzle positioned behind the coaxial gas nozzle.

Figure 5 shows the relationship between laser power and cutting speed for 76% Al_2O_3 with a thickness of 6 mm. Figure 6 shows photographs of the cut surfaces obtained with various laser powers at a cutting speed of 1500 mm/min. At a laser power of 1.8 kW, gouging occurred and cutting was impossible. Raising the laser power to 2.2 kW made cutting possible, but the temperature of the molten ceramic was so low that it was blown out

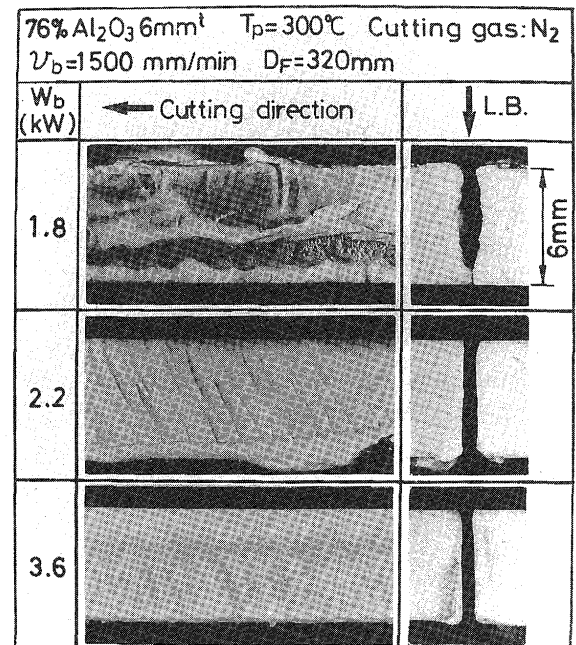


Fig. 6 Cut surface of 6 mm thick 76% Al_2O_3 at various laser powers with a cutting speed of 1500 mm/min.

forcibly by gas pressure, resulting in a rough cutting surface with a great deal of clinging dross. When the laser power was further raised to 3.6 kW, the temperature of the molten ceramic was high and dross was blown out smoothly, resulting in fine cutting without dross and a

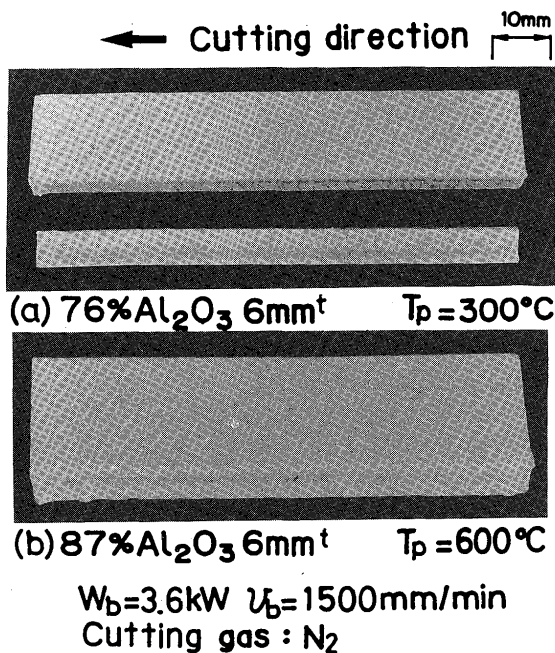


Fig. 7 Examples of fine cutting.

low degree of roughness.

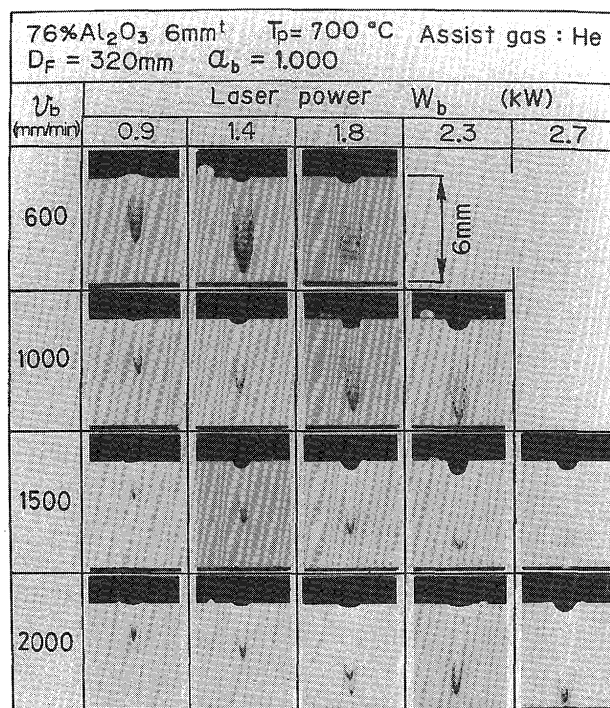
Figure 7 shows examples of fine cutting of a) 76%Al₂O₃ and b) 87%Al₂O₃. N₂ gas was used as the cutting gas, and fine cutting was possible at a preheating temperature (T_p) of 300°C for 76%Al₂O₃ and 600°C for 87%Al₂O₃.

3.2 Laser welding

Cracks often occur during laser welding of ceramics or during cooling to room temperature after welding. This is because the tensile strength of ceramics is less than 1/10 their compressive strength, and cracks are often caused by tensile stress. Since transverse cracks occur at a right angle to the weld line from the bead during the cooling process after welding, their cause is thought to be shrinkage stress after solidification. Longitudinal cracks, on the other hand, are thought to result from tensile stress restraining heat expansion in the vicinity of the bead during the heating process along on the bond or on the back of the specimen.

For these reasons, the preheating of ceramics for welding was investigated using ceramics of various alumina contents, observing whether or not cracks occurred when the preheating temperature was changed. This investigation resulted in the determination that cracks on the surface can be prevented by preheating 76%Al₂O₃ to 600°C and 87%Al₂O₃ to 800°C, and then slow cooling to 500°C in the furnace after welding. Helium gas was used as an assist gas.

The effects of laser power and welding speed on penetration depth were investigated using a beam with spot

Fig. 8 Bead cross sections of 6 mm thick 76%Al₂O₃ at various welding speeds and laser powers.

diameter of approximately 0.4 mm. Figure 8 shows bead cross sections of 6 mm thick specimens of 76%Al₂O₃ under various welding speeds and laser powers. As the laser power is increased, a typical deep penetration narrow bead is created. During partial penetration welding, small blowholes can be seen at the root of the bead cross section, and many blowholes can be seen along the bond line. Sometimes there are cracks along the bond line. As the laser power increases, there is more spatter and the bead surface shows under-fill.

When welding is carried out using a laser beam with a high energy density, there is a large amount of spatter and under-fill of the bead surface. At a high laser power and energy density, the ceramic is instantaneously heated and melted after beam irradiation. This produces a beam hole from which molten ceramic is explosively blown out to become spatter, resulting in under-fill of the bead.

In order to decrease the energy density, ceramic welding was conducted using a laser beam with a spot diameter of approximately 0.8 mm and the bead characteristics were investigated. Figure 9 shows the bead cross sections of 10 mm thick specimens of 87%Al₂O₃ under various laser powers, with a constant welding speed of 1000mm/min. The surface bead is wide, the bead is wedge-shaped, and blowholes are visible. However, there is very little spatter because of the low energy density of the beam. At a laser power of 5 kW and above the beam fully penetrates a thickness of 10 mm. At 6 kW and below there is almost

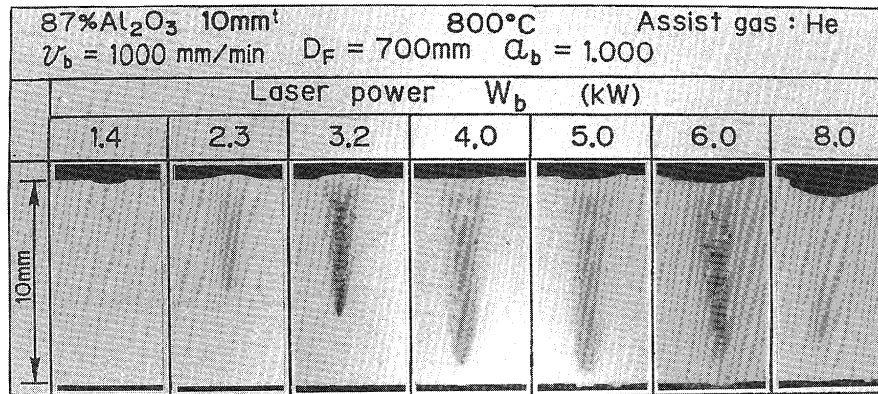


Fig. 9 Bead cross sections of 10 mm thick 87%Al₂O₃ at various laser powers.

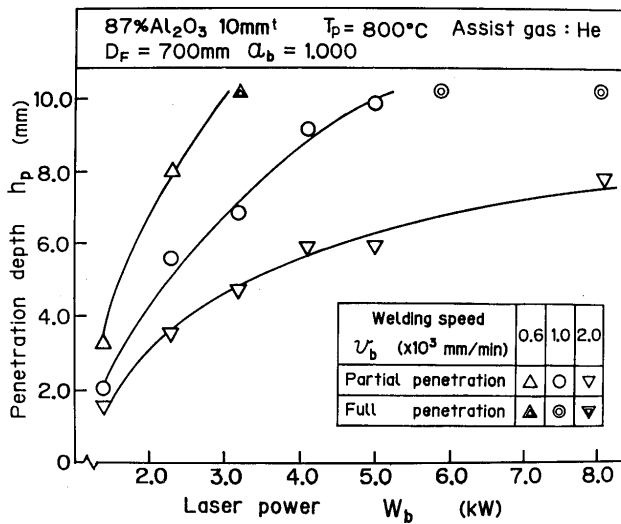


Fig. 10 Relationship between laser power and penetration depth for 10 mm thick 87%Al₂O₃ at various welding speeds.

no under-fill of the bead surface.

Figure 10 shows the relationship between laser power and penetration depth at various welding speeds using 10 mm thick specimens of 87%Al₂O₃. Compared to when the spot diameter was approximately 0.4 mm, the penetration depth is rather shallow at same laser power with a spot diameter of approximately 0.8 mm. Since increasing laser power is often accompanied by the generation of laser plasma. The penetration depth did not rise linearly with laser power, instead, there was a tendency toward saturation.

4. Conclusion

In the laser cutting of alumina ceramics, it is not possible to satisfactorily blow out molten ceramic using just a coaxial gas nozzle. However, by using a combination nozzle on 6 mm thick specimens of 76%Al₂O₃ and 87%Al₂O₃, fine cutting can be performed with a smooth cut surface and very little dross.

In regard to welding, the effect of welding speed and laser power on penetration depth in specimens of 76%Al₂O₃ and 87%Al₂O₃ was investigated. It was found that a high power laser beam with low energy density results in little spatter and little under-fill of the bead surface. It was also found that full penetration welding of 10 mm thick specimens of 76%Al₂O₃ and 87%Al₂O₃ is possible at a welding speed of 1000 mm/min and a laser power of 5–8 kW.

References

- 1) N. Aolshansky and V.M. Mesharekov: 2nd Inter. Conf. on Electron and Ion Beam Science and Technology (1966), 535–552.
- 2) J.G. Siekman and R.E. Morijn: Philips Res. Repts, **23** (1968), 367–374.
- 3) Y. Arata, H. Maruo, I. Miyamoto and S. Takeuchi: Proc. Inter. Conf. on Electron and Ion Beam Science and Technology (1976) 111.
- 4) H. Maruo, I. Miyamoto and Y. Arata: 1st Inter. Laser Processing Conf. (1981).
- 5) H. Maruo, I. Miyamoto, Y. Inoue and Y. Arata: J. of JWS, **51**–2 (1982), 182–189, **51**–8 (1982), 672–679 (in Japanese).
- 6) Y. Arata, N. Abe and T. Oda: IIW Doc. IV-374–84 (1984).
- 7) Y. Arata, N. Abe and T. Oda: Trans. of JWRI, **16**–2 (1987).